Energy Efficiency Evaluation Assessing Hydrogen Production, Energy Storage and Utilization in Integrated Alternative Energy Solutions

Rungsima Yeetsorn*‡, Chaiwat Prapainainar**, Yaowaret Maiket***

* Materials for Energy Applications group, Department of Industrial Chemistry, Faculty of Applied Science,
King Mongkut's University of Technology North Bangkok, Bangkok, Thailand

** Department of Chemical Engineering, Faculty of Engineering,
King Mongkut's University of Technology North Bangkok, Bangkok, Thailand

*** Thai-French Innovation Institute, King Mongkut's University of Technology North Bangkok, Bangkok, Thailand

rungsima.y@sci.kmutnb.ac.th; chaiwat.r@eng.kmutnb.ac.th; yaowaret.mk@gmail.com

‡ Corresponding Author; Rungsima Yeetsorn, 1518 Pracharat 1 Road, Wongsawang, Bangsue,
Bangkok 10800, Thailand

Email: rungsima.y@sci.kmutnb.ac.th

Received: 12.08.2019 Accepted: 01.10.2019

Abstract- A growing world population with rising living standards, conditions the need for ever greater levels of energy to power transports. Alternative energy technologies deliver clean energy to meet the needs of the world in terms of transportation. The integration of alternative energy generators is an interesting perspective to prevent issues at the levels of hydrogen supply and energy balance. Additionally, efficiency, storage, and utilization of energy systems play an important role in the consumption of energy. In the current study, the comparative evaluation addressing energy efficiency between hydrogen production via an electrolytic process and hydrogen utilization in a proton exchange membrane fuel cell (PEMFC), was investigated using a simulation model. Hydrogen gas was produced from water via electrolysis using alternative energy resources deriving from wind turbines and solar cells. The produced hydrogen gas was compressed and stored under high-pressure conditions, before being supplied to PEMFCs in the frame of electricity production for the purpose of application to an electric vehicle. The hydrogen production and storage solutions derived from wind energy-wind/hydrogen and from solar energy-solar/hydrogen were created on the basis of process simulation models prior to the calculation of both the hydrogen production rate via electrolysis and the energy efficiency value. Subsequently, the utilization of hydrogen energy by PEMFCs was also examined, and the simulation of the fuel cells powered by pressurized hydrogen, was performed to compute the energy efficiency as well. The simulation models of two processes were described in details while the assumptions underlying the calculations appear along. The overall efficiency levels of wind/hydrogen/electricity and solar/hydrogen/electricity systems reported in this work, bestow technical capability for implementation, and the experimental models arguably demonstrate the feasibility of integrating alternative energy technologies to support the growth of modern automotive technologies.

Keywords Energy efficiency, PEM fuel cell, Alternative energy, Wind energy, Electrolyzer, Solar energy

1. Introduction

Presently, the laudable aspects associated with the production of energy from alternative energy resources, have received world attention. It is extensively documented that the combustion of petroleum or fossil fuels is detrimental to the environment and human health [1]. Cleaner energy generators play an imperative role in the resolution of this problem. The three main dimensions determining the selection of appropriate energy resources by researchers and

engineers, depend on whether, supplies are sustainable, the total value of energy per unit of volume is high, and the release of energy to produce useful work is done without combustion (Shell Global, 2018). Along those dimensions, hydrogen qualifies as an adequate energy source; hence it constitutes a decent fuel for modern technologies such as electric vehicles. An energy conversion device utilizing hydrogen to generate drive shaft work directly, is a fuel cell (FC). As known, an FC is an electrochemical device converting chemical energy into electrical energy [2]. It should be noted that the fuel cell used in this research is a proton exchange membrane fuel cell (PEMFC). In a PEM fuel cell, the hydrogen gas is electrochemically oxidized on an anode catalyst (Platinum: Pt) layer, and then the hydrogen gas is dissociated to produce protons and electrons. The protons are directed to the proton conductive membrane through which they pass to the cathode side, whereas the electrons are transferred via the outer circuit to reach the cathode side. The protons and electrons react with the oxygen gas on the surface of a cathode catalyst (Pt) to initiate a reduction reaction, and the overall reaction is called a redox reaction [3]. The major concern in opting for FCs at the center of an effective commercialization of modern electric vehicles, is about hydrogen production, storage and distribution. Dominant technologies for hydrogen production are: steam reforming of hydrocarbons, electrolysis and thermolysis. In Thailand, hydrogen gas can be mainly produced via the reforming process of natural gas produced from petroleum refineries. Three major hydrogen distribution solutions are: cylinder packs, liquid hydrogen lorries, and supply pipelines (Hydrogen Europe, 2017). The transport of compressed gaseous or liquid hydrogen by lorry and/or by pipeline to selected locations, are the global transport options used. As the investment costs relative to the construction of infrastructures for a pipeline network are quite high, the Thai government is expected to show awareness as to cost effective possibilities involving this investment. This work aims at demonstrating a hydrogen gas distribution alternative termed "Onsite Gas Generation Solution". The onsite gas generation solution presented in this work is an alternative energy/electrolyzer system. An electrolysis process lets water molecules absorb electrical energy and dissociate into hydrogen and oxygen gases. This process is reversible as the process induced by a fuel cell, namely a galvanic process, activates the recombination of hydrogen and oxygen, which results in the formation of water and the release of the absorbed energy. However, it is difficult to accomplish a mix of desirable energy balance combined with cost-effectiveness when FCs utilize hydrogen, produced by an electrolysis method, as an oxidative fuel to generate electricity. The integration of alternative energy resources, such as wind or solar energy, is the process of power transfer from an alternative energy resource to a utility system. It implies that wind or solar energy is the primary source of electricity [4]. Wind and solar energies are predicted to account for 40% of the world energy production by 2060, and the sun will become an enormous energy generator in decades to come [3]. Unfortunately, the production of energy deriving from wind and solar sources, relies on uncontrollable weather-contingent factors, since power generation from wind turbines and solar cells are inherently intermittent and inconstant [5]. Thus, they cannot be used to provide energy in a consistent manner. The integrated energy approach mentioned earlier, rests upon the concept of synergism wherein separate units act simultaneously and in coordination. This approach provides a level of efficiency greater than that obtained by the sum of the individual units. likewise, an energy storage device can be adopted and hence identifies itself as the ultimate solution to increase the stability of the energy production system [6]. The energy storage systems can be divided into six categories: mechanical energy storage, electrochemical energy storage, chemical energy storage, electrical energy storage, thermal energy storage, and hybrid energy storage systems [7]. An electrolyzer is an energy storage device that can transform electrical energy into chemical energy in the form of hydrogen and oxygen gases which can be employed by the FC for electricity generation [8-12]. There exist various types of electrolyzers, notably the proton exchange membrane electrolyzer (PEME), the alkaline electrolyzer and the solid oxide electrolyzer [5]. The complete reaction in the electrolyzer is of a redox type via an electrolytic process [13]. Research work related to the use of a multi-energy-source technology to generate electricity has gained attention from researchers over the years. For instance, the electricity supply directed to the homogeneous charge compression ignition (HCCI) chamber of the fuel cell, was generated via the integrated solar cell/electrolyzer system [14]. This system provided 14.7% of energy efficiency when the cooling system was excluded. When the system included the cooling system, the efficiency was 20.7%. Ganguly et al. [15] created a fuel cell hybridization system (solar cell/electrolyzer/fuel cell system) as an electricity generator for a floricultural greenhouse with a fan and pad cooling system. The system consisted of 51 solar panels, a 3.3 kW electrolyzer, and two PEMFC stacks delivering 560 W of power. Concerning the application of hybridization systems to electric vehicles, Huang et al. [16] advocated a hybridization system of cell/wind turbine/electrolyzer for the production of hydrogen. Operating factors such as temperature, hydrogen flow rate, and Faraday efficiency of the electrolyzer, were computed using the mathematical simulation available through MATLAB/Simulink. The described system delivered a power output amounting to 30 kW. Comparisons between the different multi-energy-source systems in terms of energy efficiency and cost, were approached by Khalid et al. [17]. The systems evaluated in their work were hydrogen/wind, turbine/electricity and hydrogen/PEMFC systems, generating power for a building in Canada. Results indicated that the energy efficiency levels of the hydrogen/wind and turbine/electricity systems (20.7%) were lower than those of the hydrogen/PEMFC system (24.7%). On the other hand, the cost of electricity generation via the hydrogen/wind and turbine/electricity systems (0.431 $/kWh), was higher than that via the hydrogen/PEMFC system (0.387 $/kWh). Buonomano et al. [18] reported the simulation of the wind and solar energy hybridization system for the design of a renewable plant. The system provided 200 kW of electrical power consisting of 190 kW from solar panels and 10 kW from a wind turbine. Based on the literature review laid out above, the integration of onsite hydrogen gas generation combined to electrical generation in set-ups, such as the

wind/electrolyzer/PEMFC or the solar/electrolyzer/PEMFC systems, has been less investigated.

In this article, the integration of alternative energy technologies, power generation solutions, and energy storage technologies (hydrogen storage), was demonstrated via a computational simulation focusing on its application in the electric vehicle segment. The specifications of the car Toyota Mirai, which is a hydrogen fuel cell electric vehicle (FCEV), served as simulation data for this study. The Mirai which has an electric drivetrain and a traction battery, is a sedan-like vehicle to be used as a city car. In the set-up of this research, electricity generated from wind turbines or solar cells as a primary source of energy, was delivered for the purpose of producing hydrogen gas through an electrolyzer. The produced hydrogen was subsequently transferred to a PEMFC stack in the FCEV. The set-up is arranged in parallel with the simulation model of Aspen plus V.7.3 as a myriad of factors significantly affect efficiency performance in the cycle of energy generation.

2. Methodology

The conceptual idea of this research resides in the investigation of the different linkages between the production of electricity from primary energy resources, the production of hydrogen gas via an electrolytic process, and the generation of electricity by PEMFCs. The experimental procedure ponders upon calculations in conjunction with simulations to balance mass and energy along the system. Results answered the research question concerning the quantification of the necessary power to be generated by PEMFCs when wind turbines and photovoltaic cells constitute primary energy sources. In the preliminary steps, it was imperative to know the energy efficiency values of selected devices in order to establish the fundamental data required for determining the relations between electricity consumption engendered by both energy sources, hydrogen production, and power generation by the PEMFCs.

The calculations in the simulation steps were based on the assumption that two integrated power generation systems (a solar cell/electrolyzer and a wind/electrolyzer) would consistently produce 38.7 kmol of hydrogen gas to supply the Toyota Mirai. The value obtained as for the amount of produced hydrogen gas depended on the fuel consumption of the Toyota Mirai required to cruise at a constant speed (km/hr) for 6.035 hours. The schematic illustrating the concept of this research is exhibited in Fig. 1, and the specifications of the hydrogen cylinder used to store the produced hydrogen before supplying the Toyota Mirai, are presented in Table 1.

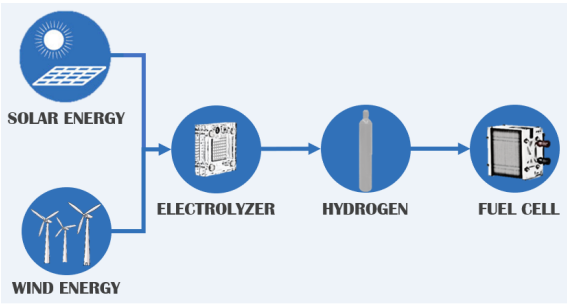

Fig. 1. The concept of this research

Table 1. Specifications of the hydrogen cylinder

The hydrogen cylinder	
Volume (on label)	7 m^3 at STP
Height	1.34 m
Circumference	0.723 m
Diameter	0.23 m
Volume	56.52 L
Pressure	2,000 psig
Temperature	300 K

The schematic of the overall process, which used a wind turbine as a primary power source, is displayed in Figure 2.

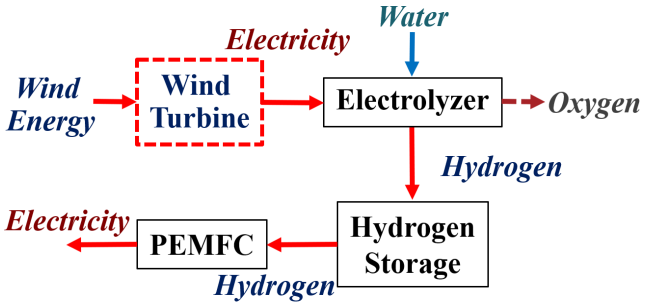

Fig. 2. The overall process of electricity production initiated by a wind turbine.

According to the schematic diagram in Fig. 2, the primary source is a wind turbine transforming wind energy into electricity. The shaft of the turbine is connected to an electricity generator which uses the rotary motion of the shaft to impart rotational energy to a rotor which has oppositely charged magnets and is surrounded by copper wire loops. The rotor spinning around the inside of the core, creates electromagnetic induction to generate electricity [19]. The electricity produced by the wind turbine is utilized for hydrogen production. The passage of the produced electric current through the electrolyzer results in the decomposition of water into oxygen and hydrogen gases. The hydrogen storage device acts as a depository where hydrogen gas accumulates for the further purpose of supplying the stack of PEMFCs. A PEMFC is a device for converting chemical energy into electrical energy so as to power an EV or a hydrogen car.

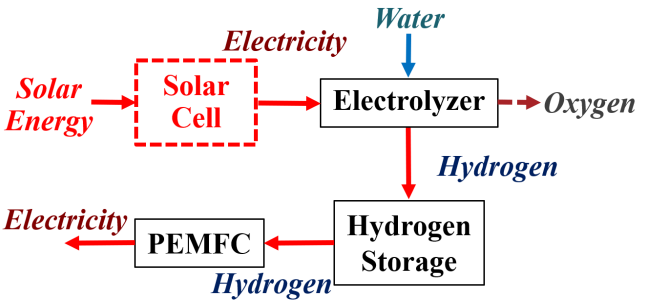

Fig. 3. The overall process of electricity production initiated by a solar cell.

In the configuration of solar energy being transformed into PEMFC electricity, the hydrogen production process requires solar energy as the resource to start the cycle. In Fig. 3, the solar energy is converted by photovoltaic cells through a process comprising two distinct steps. First, a semiconductor

in the cells absorbs the solar energy, which conditions the creation of electron-hole pairs. Then, electrons are separated into negative terminals, while holes are separated into positive ones. As a result, electrical power is finally generated [20-22]. In principle, this process is comparable to that of wind energy being transformed into PEMFC electricity, but the dissimilarity between the two processes resides in the nature of the primary energy resource. Fig. 3 illustrates, through a schematic, the electricity generation process using solar energy as a primary power resource.

It is important to note that interconnection among devices usually involves energy losses, due for instance to electrical wire resistance, contact resistance, and energy transformation. Nevertheless, the scope of the different computations in this work are predicated on the proposition that these losses are negligible, due to the fact that interconnections among the units after generating electricity from primary sources (wind turbines or solar panels), are identical in both systems.

2.1 Wind energy to PEMFC electricity

Wind power or the amount of wind energy as a function of time, was calculated from the basic equation describing the kinetic energy of wind moving at a particular speed (W), as in Equation (1).

$$W = \frac{1}{2}(\rho \upsilon A)\upsilon^2 \quad (1)$$

The electrical power produced from the wind turbine was calculated using the equation describing the performance coefficient or the power efficiency of a wind turbine (Cp) which is the ratio of the available electrical power generated by the wind turbine to the wind power as only a fraction of the kinetic energy of the wind can be converted into mechanical energy revolving a rotor.

$$C_P = \frac{W_E}{W} \quad (2)$$

Therefore, the available electrical power generated by the wind turbine was calculated from

$$W_E = \frac{1}{2}(\rho A)\upsilon^3 C_p \quad (3)$$

where W is the wind power, m is the mass of wind in motion considering the rates of both mass flow and change of distance since the power of the wind refers to the rate of change of energy, which are expressed by

$$E = \frac{1}{2}m\upsilon^2 \quad (4)$$

$$\rho A\upsilon = \frac{dm}{dt} \quad (5)$$

$$\upsilon = \frac{dx}{dt} \quad (6)$$

So ρ is the air density, A is the cross-sectional area of the wind turbine, Cp is the power efficiency of the wind turbine, t and x refer to time and distance accordingly, υ is the velocity of wind, and W_E is the electrical power [23-24]. The proton exchange membrane (PEM) electrolyzer pioneered by Ekin Ozgirgin and his team [23] was the electrolyzer model selected for this simulation, since general information concerning the equations needed to perform calculations was provided. The specifications of the PEM electrolyzer are shown in Table 2.

Table 2. The specification of PEM electrolyzer [23]

PEM electrolyzer	
Cell area	400 cm^2
Cell number	15
Current density	0.5 A/cm^2
Membrane	Perfluorosulfonate acid
Design voltage	24 V
Maximum power	4,700 W

The electrical performance of the PEM electrolyzer (η_{elec}) was computed via a multiplication of current efficiency (η_i) with voltage efficiency ($\eta_{voltage}$) [14-15]. This study assumes 88% voltage efficiency, and then current efficiency can be calculated from Equation (7-8).

$$\eta_{elec} = (\eta_i)(\eta_{voltage}) \quad (7)$$

$$\eta_i = 96.5\left[\exp\frac{0.09}{i_{elec}} - \frac{75.5}{i_{elec}^2}\right] \quad (8)$$

where i_{elec} is the current passing through the electrolyzer cells; i_{elec} directly varies with cell area, cell number, and current density. When the value of i_{elec} is 3,000 A, results indicate that η_i and η_{elec} are equal to 96.5% and 84.9% respectively [20-21]. Relevant data referring to the research work by Ekin Ozgirgin, et.al [23], were applied to the construction of a model for determining PEMFC efficiency. The mathematical equations used in this case correspond to the electrical power and heat duty involved in the fuel cell operation. The key criteria relative to the operation of the PEMFC in this work, are mentioned in Table 3.

Table 3. Information concerning the PEMFC operation.

PEMFC	
Current density (at 0.6 V)	1 A/cm^2
Type of membrane	Nafion 212
Cell area	50 cm^2
Cell number	40 cells
Maximum power	1,200 W

2.2 Solar energy to PEMFC electricity

The system transforming solar energy to PEMFC electricity was similar to that transforming wind energy to PEMFC electricity at the exception of the primary energy captured through either solar photovoltaic cells or wind turbines, as displayed in Fig. 2, to initiate the entire process. To finalize calculations, following seven parameters were considered. The nuclear fusion reactions happening in the sun release approximately 3.47×10^{24} kJ/s of energy, of which a small part is irradiated onto the earth's surface, hence the application of the solar constant (1,353 W/m^2) to the simulation. This value constitutes the flux density of mean solar radiation from the Sun onto the Earth whose average distance is estimated at 1.5×10^{11} m. Importantly, the

reflected radiation also needs to be taken into account. The radiation from the Sun directly reaches the Earth's surface, but it is partly reflected back to the atmosphere before going out into space. The reflected solar radiation percentage is about 30% (≈1,353 W/m^2). The amount of energy irradiated by the Sun depends on the distance and angle between the Earth and the Sun as calculated in Equation (9),

$$I_0 = I_{SC}\left[1 + 0.033\cos\frac{360\,N}{365}\right] \quad (9)$$

where I_0 is the irradiance on a plane perpendicular to the rays of the sun outside the atmosphere, I_{sc} is the solar constant (1,353 W/m^2), and N is the Julian date. Assuming that the world is perfectly spherical, the average irradiance at the Earth's surface is equal to 250 W/cm^2. On an annual basis, the average irradiance from the Sun outside the Earth's atmosphere is approximately 1,353.031 W/m^2. On the premise that the solar radiation which is reflected by the ground (reflectivity) averages 30%, the irradiance value amounts to 947.121 W/m^2.

3. Results and discussion

3.1 The efficiency of wind energy converted into PEMFC electricity

Regarding the design requirements described in the schematic of the electricity generating process using a wind turbine as a primary power source (Fig. 2), the efficiency as for the conversion process of wind energy into PEMFC electricity, was calculated by multiplying each and every device's efficiency value so as to come up with the overall energy efficiency value for the entire energy transformation system composed of the wind turbine, the electrolyzer, and the stack of PEMFCs. Four types of wind turbines; simple, dual-rotor, Darrieus, and Savonius (Fig. 4), commercialized in Thailand, had been selected to undergo evaluation, as part of the simulation process whereby energy transfers were assessed along all phases of transformation, from the wind turbine to the PEMFC stack. A popularly common wind turbine in Thailand is the simple turbine with 100 m^2 of swept area and 11.28 m of diameter generating 3,231.334 W of electrical power with 32% of energy efficiency (dependent upon wind velocity).

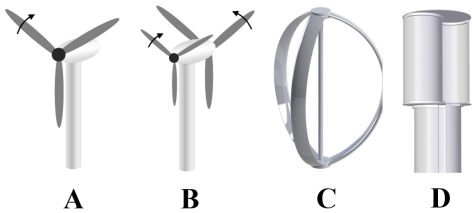

Fig. 4. Types of wind turbines A) simple [25] B) dual-rotor [25] C) Darrieus [26], and D) Savonius [27].

It is worth noting that to calculate the actual work efficiency of any system, work and energy losses from the different units (wind turbine, electrolyzer, PEMFCs, and load) in the integrated system are typically concerned, but the losses occurring in this process were disregarded. The reason leading to this assumption, stems upon the fact that the objective of this work is to primarily study the feasibility of producing hydrogen gas from an alternative resource. The efficiency losses inherent in the functioning of a wind turbine, typically comprise the tip loss, wake effect, drivetrain loss, and simplification-contingent blade shape loss. Generally, wind turbines are designed in a variety of shapes which tend to reduce losses and thus improve efficiency. The simple turbine with 3 blades is labeled as a horizontal-axis wind turbine (HAWT) and yields a peak energy efficiency of 50%, whereas the dual-rotor turbine is labeled as a vertical axis wind turbine (VAWT) which uses drag propulsion. The dual-rotor turbine achieves an efficiency level of 20%. The Darrieus turbine falls under the VAWT category and uses lift propulsion, while it provides a peak energy efficiency of 40%. The Savonius turbine which delivers a peak energy efficiency of 16%, is classified as a VAWT and uses drag propulsion [28]. Simulation results (refer to Table 4) show that electrical power and efficiency of a wind turbine (Cp) are impacted by the turbine configuration. When the turbines run at a wind velocity of 5.6 m/s, the efficiency of most turbines is situated in the range 32-37%, except the Savonius model.

Table 4. Data pertaining to different types of wind turbine.

Parameters	Types of wind turbine			
	Simple	**Dual rotor**	**Darrieus**	**Savonius**
Diameter (m)	11.28	3.75	2.89	0.96
Installation area (m^2)	3.31	11.05	5.96	0.92
Wind power (W)	0.480	0.343	0.221	0.022
Cp	0.32	0.30	0.37	0.23
Wind velocity (m/s)	5.6	5.6	5.6	5.6
Electrical power (W)	106.96	334.75	222.68	21.37

The dual-rotor turbine provided the highest electrical power (334.75 W), whereas the Savonius turbine gave 21.37 W of electrical power, which was the lowest value. In awareness that a rotor extracts kinetic energy from wind and converts it into rotational energy, this poor performance was mainly attributed to the fact that the dual-rotor turbine consists of six blades which register the highest value in terms of surface area in contact with air. It is worth noting that vertical-axis wind turbines are capable of capturing wind energy from all directions due to their omni-directional design [29] The impediment to this functionality is the fact that their efficiency may be decreased if negative torque is generated as a result of the rotors revolving swiftly. Wind speed distribution and direction of motion differ as a function of location, therefore in order to maximize the energy output, the design of wind turbines necessarily needs to be adapted to the specificity of the characteristics defining a particular site.

In the matter concerning the electrolyzer, its efficiency depended upon the relation linking used electrical energy and heat duty in the process of water dissociation, as expressed in Equation (7). Obtained results derive from the computation of data determining efficiency through the

simulation program (Aspen Plus) as shown in Tables 5 and 6. This study performed simulations following predicated assumptions while using mmol/s as a unit of measurement. Results indicated an average H_2O conversion value of approximately 0.906. The constant value in Equation (10) was set according to the voltage value of a PEM electrolyzer, considered as ideal.

$$\%Eff_{elec} = \frac{\text{Heat duty}}{\text{Power consumption}} \text{x} 100\% \text{ x } 1.232 \quad (10$$

Table 5. Reference electrolysis data [23]

H_2O consumption (L/min)	H_2 production (L/min)	O_2 production (L/min)	Power consumption (W)
0.0027	3.04	1.50	938
0.0050	6.09	3.04	1,875
0.0080	9.13	4.56	2,813
0.0110	12.17	6.09	3,750
0.0134	15.21	7.61	4,688

Table 6. Simulation-derived results for the electrolyzer using the Aspen Plus program

H_2O Consumption (mmol/s)	Production		Heat duty (W) (at 1 bar, 25 °C)	H_2O conversion	Efficiency (%)
	H_2 (mmol/s)	O_2 (mmol/s)			
2.500	2.227	1.113	644.86	0.891	84.70
4.638	4.469	2.235	1,293.77	0.964	85.01
7.421	6.701	3.350	1,940.30	0.903	84.98
10.204	8.932	4.466	2,586.36	0.875	84.98
12.430	11.163	5.581	3,232.42	0.898	84.95

$$\%Eff_{FC} = \frac{\text{Electrical power} + \text{Released heat}}{\text{Heat duty}} \text{x} 100\% \quad (11)$$

$$\%Eff_{FC^*} = \frac{\text{Electrical power}}{\text{Heat duty}} \text{x} 100\% \quad (12)$$

PEMFCs characteristically produce two main types of energy, electrical and thermal energy, so electrical power and heat release were taken into account in the determination of the PEMFC efficiency as in Equations (11) and (12). Obtained results derive from the computation of data determining efficiency using the simulation program (Aspen Plus) as shown in Tables 7 and 8. This study performed simulations while using mmol/s as a unit of measurement.

Table 7. Reference PEMFC data [23]

H_2 consumption (L/min)	O_2 consumption (L/min)	PEMFC power output (W)	Heat release (W)
3.04	1.52	200	344
6.10	3.04	400	687
9.13	4.57	600	1,030
12.17	6.09	800	1,373
15.22	7.61	1,000	1,717

Table 8. Simulation-derived results for the PEMFC using the Aspen plus program

H_2 consumption (mmol/s)	O_2 Consumption (mmol/s)	Feed conditions: 1 bar, 80 °C Reaction conditions: 1 bar, 80 °C		
		Heat duty (W)	$\%Eff_{FC}$	$\%Eff_{FC^*}$
2.231	1.101	637.279	85.36	31.38
4.469	2.231	1,278.843	85.00	31.28
6.701	3.347	1,914.122	85.16	31.35
8.932	4.469	2,551.401	85.17	31.36
11.163	5.585	3,190.680	85.15	31.34
Average efficiency			85.05	31.34

Two types of efficiency, $\%Eff_{FC}$ and $\%Eff_{FC^*}$, were evaluated through simulation in this research. The $\%Eff_{FC}$ was calculated from the ratio of electrical and heat energy values to the heat duty one, whereas, the $\%Eff_{FC^*}$ was computed by dividing the produced electrical power by the heat duty. The average efficiency values ($\%Eff_{FC}$ and $\%Eff_{FC^*}$) were 85.06% and 31.34%, respectively.

The efficiency of the wind/electrolyzer/PEMFC system ($\%Eff_{WFC}$) was calculated from Cp, $\%Eff_{elec}$, and $\%Eff_{FC^*}$. While evaluating the efficiency of the electrical energy conversion process, the simulation calculations ignored the heat released by the PEM fuel cell. Thus, $\%Eff_{FC^*}$ was representative of the PEMFC efficiency described in Equations (13) and (14). In summary, the efficiency values of the wind turbine, the electrolyzer, and the stack of PEMFCs were approximately 32%, 85%, and 31% respectively. Therefore, the overall efficiency of the system wind/electrolyzer/PEMFC was around 9% as shown in Fig. 5.

$$\%Eff_{WFC^*} = \frac{\text{Electrical power}}{\text{Wind power}} \text{x} \frac{\text{Heat duty}_{\text{Electrolyzer}}}{\text{Power consumption}} \text{x} \frac{\text{Electrical power}}{\text{Heat duty}_{\text{Fuel cell}}} \text{x} 100\% \quad (13)$$

$$\%Eff_{WFC} = \frac{\text{Electrical power}}{\text{Wind power}} \text{x} 100\% \quad (14)$$

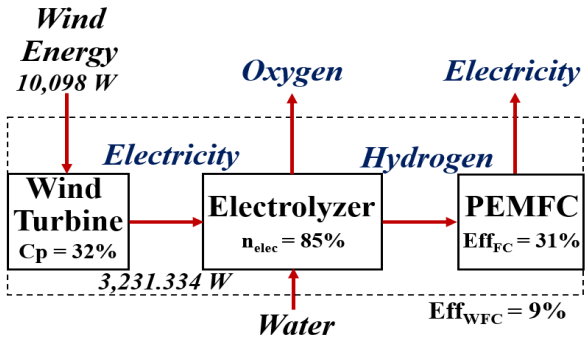

Fig. 5. Efficiency diagram of the system wind/electrolyzer/ PEMFC

3.2 The efficiency of solar energy to PEMFC electricity

The efficiency of the solar/electrolyzer/PEMFC system was calculated similarly as in the simulation for the wind/electrolyzer/PEMFC one. The solar panels comprise a variety of different sizes and areas as shown in Fig. 6 and Table 9. The commercial modules of solar panels A, B, and

C, include polycrystalline silicon, monocrystalline silicon, and amorphous silicon types. The monocrystalline silicon panels are built from single-crystal silicon formed into bars which are thereafter cut into wafers. A wafer incorporating a single continuous crystal improves the flow of electrons making the efficiency of monocrystalline solar panels superior to that of polycrystalline solar ones (Energysage, 2018). In the case of solar panels integrating amorphous silicon, their production involves a process, known as chemical vapor deposition, during which thin film layers of silicon (Energy informative, 2014) [30], belonging to the direct band gap class, are grown. In this research, the solar panel A constituted the basis for our study since it was representative of the solar panel type widely manufactured for the market in Thailand.

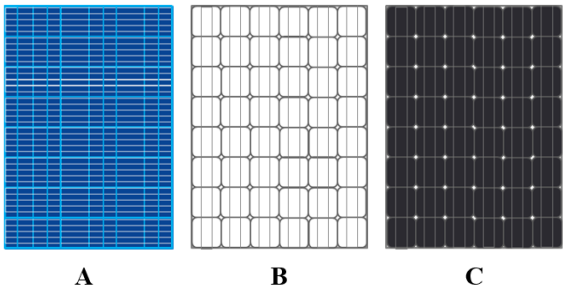

Fig. 6. The various types of solar panels: A) Polycrystalline solar panel, B) Monocrystalline solar panel, and C) Amorphous solar panel.

Table 9. Comparison between specifications of different types of solar panels

Specifications	Panel Samples		
	A	B	C
Size (WxLxD) (m^3)	1.480x0.665 x0.035	1.481x0.666 x0.048	1.16x0.668 x0.035
Area (m^2)	0.9842	0.9863	0.7749
Max. voltage (V)	34.40	17.82	17.30
Max. current (A)	3.78	7.30	8.00
Max. power (W)	130	130	130
Power/Area (W/m^2)	132.09	131.81	167.76
Efficiency	0.132	0.132	0.168
Price (THB/W)	19.70	23.83	21.92

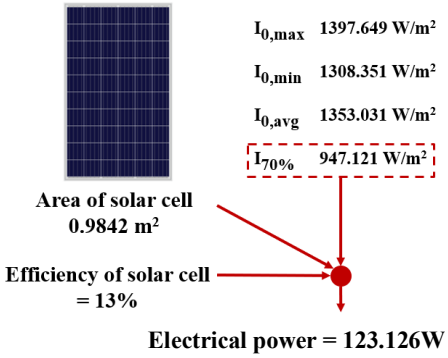

Fig. 7. Electrical power from solar energy

Fig. 7 illustrates the flow that the calculation process followed to compute the electrical power on the basis of the data relative to the solar panel A which combines highest voltage and lowest cost. With an irradiance value of 947.121 W/m^2, all relevant data were inputted so as to calculate the overall efficiency of the solar/electrolyzer/PEMFC system as shown in Fig. 8.

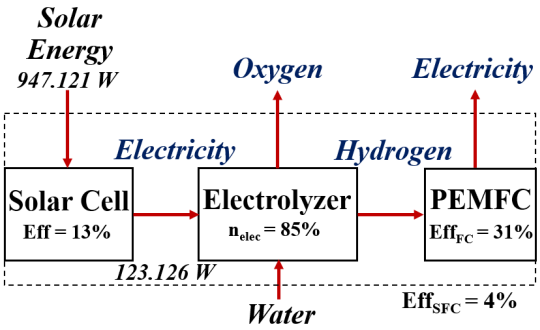

Fig. 8. Efficiency diagram of the system solar/electrolyzer/ PEMFC

3.3 Electrical energy balance

The produced hydrogen gas may be directly supplied to the stack of PEMFCs or stored in a gas cylinder. This energy-wise study proceeded with the storage of 7 m^3 of hydrogen in a standard gas cylinder at STP (Table 1) prior to the injection of hydrogen gas into the group of PEMFCs. It is important to note that the pressurized unit which is normally installed to compress gas into the cylinder with a pressure of 2,000 psig, was not included in this simulation. The assumption was made that the hydrogen flow rate, which was fixed for the feeding of hydrogen fuel into the PEMFCs, was equivalent to the hydrogen production rate of the electrolyzer. The simulation results in Table 10 indicate that using one wind turbine as a primary energy source, generates sufficient electrical power output, amounting to 3,231.334 W, to produce hydrogen gas fuel from an electrolyzer. In terms of performance, the wind/electrolyzer/PEMFC system managed to generate an electrical power output of approximately 688.570 W.

Table 10. Simulation results for the wind/ electrolyzer/ PEMFC system

Parameters	Wind turbine	Electrolyzer	PEMFC
Wind energy (W)	10,098	-	-
Electrical power output (W)	3,231.334	3,231.334	688.570
Heat duty (W)	-	2,227.312	2,197.085
H_2 flow rate (mmol/s)	-	7.6916	7.6916

Thus, the findings for the solar/electrolyzer/PEMFC system (Table 11), show that one photovoltaic cell panel cannot generate sufficient electricity to drive an electrolysis reaction; hence ten panels are required to generate the 1,231.260 W required for producing hydrogen gas through an electrolyzer. The electrical power output (688.570 W) was generated by the wind /electrolyzer/PEMFC system using one wind turbine rotating at 5.6 m/s of wind velocity.

In order to obtain the same PEMFC power output (688.570 W), the solar/electrolyzer/PEMFC system needs to contain 26-27 solar panels.

Table 11. Simulation results for the solar/electrolyzer/PEM FC system

Parameters	Solar cell (10 units)	Electrolyzer	PEMFC
Solar energy (W)	947.121	-	-
Electricity power output (W)	1,231.260	1,231.260	262.370
Heat duty (W)	-	848.690	837.175
H_2 flow rate (mmol/s)	-	2.9308	2.9308

Finally, the produced hydrogen gas was supplied to the Toyota Mirai car as the projected earlier (H2 Mobility Deutschland GmbH&Co.KG, 2019). The car uses 370 solid polymer electrolyte fuel cells which are gathered in a stack, to provide a maximum output voltage of 114 kW. In fact, Mirai consumes 2.48 kmol or 5 kg of hydrogen to cover a distance of 300 miles. Since this range is achieved with a full tank (5 Kg), calculations estimate that the Mirai runs out of fuel after 6.035 hours of driving elapse, when it cruises at a speed of 80 km/hr. The results shown in Table 12 indicate that the wind/electrolyzer/PEMFC system consisting of 15 wind turbines, takes 5.971 hours to fully fill hydrogen gas into the Mirai at a flow rate of 115.374 mmol/s whereas the solar/electrolyzer/PEMFC set-up comprising 39 solar panels, needs 6.027 hours to fully fill hydrogen into the Mirai at a flow rate of 114.301 mmol/s. It implies that the wind/electrolyzer/PEMFC system notably provides higher performance in comparison to the solar/electrolyzer/PEMFC one. However, the wind/electrolyzer/PEMFC configuration was considered inferior to the solar/electrolyzer/PEMFC one as far as installation area requirements and costs are concerned.

Table 12. Comparative analysis of configurations integrating different primary power sources

Energy source	Wind turbine	Solar cell
No. of unit	15	39
Electricity power (W)	48,470.01	48,019.14
Heat duty (W)	33,409.69	33,098.91
H_2O Consumption (mmol/s)	127.3305	126.1455
H_2 production (mmol/s)	115.374	114.301
Heat duty Aspen (W)	33,409.46	33,098.52
Time (hours)	5.971	6.027
Installation area (m^2)	49.65	38.38
Cost (THB)	606,600	99,879

Table 13. Power generated by a wind turbine on the basis of wind velocity for each region of Thailand (NAJUA, 2019)

Region of Thailand	Wind velocity (m/s)	Power generated from wind (W)
North (Chiang Mai)	0.347	6.628
Northeast (Khon Kaen)	0.140	2.674
Central (Bangkok)	0.520-0.620	9.932-11.842
East (Chanthaburi)	0.100	1.910
West (Kanchanaburi)	0.080	1.528
South (Phuket)	0.290	5.539

Table 14. Power generated by a solar panel on the basis of solar irradiance for each region of Thailand (Ministry of Energy, 2017)

Region of Thailand	70% of solar irradiance (MJ/m^2-day)	Power generated from solar irradiation (W)
North (Chiang Mai)	10.319	275.399
Northeast (Khon Kaen)	11.925	318.261
Central (Bangkok)	9.610	256.477
East (Chanthaburi)	10.455	279.029
West (Kanchanaburi)	14.482	386.504
South (Phuket)	11.835	315.859

This section presents the simulation cases of a simple turbine and a polycrystalline solar panel, which were oriented towards the application of multi-source power generators, so as to produce hydrogen gas for electric vehicles in big cities of Thailand (Tables 13 and 14). The selected simple wind turbine which contains a propeller with a diameter of 11.28 m, requires an installation area of 3.31 m^2, and costs 40,440 THB. When this turbine rotates at a wind velocity of 0.520-0.620 m/s, it generates an electrical power around 9.932-11.842 W. In the other case, the polycrystalline solar panel with an active area of 0.984 m^2, has a price tag of 2,561 THB and needs an installation area of 0.984 m^2. The electrical power output of 256.477 W, was generated as a result of solar irradiation providing an irradiance estimated at 9.610 MJ/m^2. The results suggest that solar panels are suitably adapted for the production of electrical power, intended at supplying fuel cells of electric vehicles, in a metropolis like Bangkok

4. Conclusions

The automotive industry has invested considerable effort towards the commercialization of "cars for the future: fuel cell electric vehicles" which are expected to eventually possess the necessary capabilities to compete with internal combustion engine vehicles. In reality, cars for the future cannot be significantly developed without considering alternative energy and energy storage technologies. This work demonstrated the viability of integrating alternative energy and energy storage technologies serving the purpose of power generation for which computational simulation

assisted the provision of solutions. This study has drawn the following conclusions:

- The efficiency values of the wind/hydrogen/electricity and solar/hydrogen/electricity systems were approximately 9 % and 4 %, respectively.
- Utilizing one wind turbine for the wind/hydrogen/ electricity system provided 688.57 W of overall electrical power output, which indicated an adequate and positive energy balance.
- The use of one solar cell panel failed to generate sufficient power for operating the electrolyzer, hence ten panels were required to activate the solar/hydrogen/electricity system. The overall electrical power output generated by this system was only 262.37 W.
- The wind/electrolyzer/PEMFC system provided a performance higher than that of the solar/electrolyzer/ PEMFC one.
- The solar/electrolyzer/PEMFC system was superior in comparison to the wind/electrolyzer/PEMFC one, when considering costs and installation area requirements.

In order to succeed in shifting use from fossil fuels to alternative energy resources, it is indispensable to resort to a utilization of multi-power sources, which is predicated upon the consideration of energy balance.

Acknowledgement

The authors gratefully acknowledge the support of Mr. Nutthawoot Jermkwan for his contribution to this project.

References

[1] D. Icaza, and M. Avila, "Modeling and Simulation of a Solar System in the Quingeo Church in Ecuador", In 2018 International Conference on Smart Grid (icSmartGrid). IEEE, pp. 158-163, 2018.
[2] The national renewable energy laboratory (NREL), "Renewable Energy: An Overview", Energy efficiency and renewable energy, pp. 1-8, 2001.
[3] N. Alrikabi, "Renewable Energy Types", Journal of Clean Energy Technology, pp.1-4, 2014.
[4] H. Dida, and M. Bekhti "Study, modeling and simulation of the electrical characteristic of space satellite solar cells", In 2017 IEEE 6th International Conference on Renewable Energy Research and Applications (ICRERA). IEEE. pp. 983-987, 2017.
[5] A. Mohammadi, and M. Mehrpooya, "A comprehensive review on coupling different types of electrolyzer to renewable energy sources", Energy, pp. 632-655, 2018.
[6] M. Lindsay, and R. Carriveau, "A review of energy storage financing—Learning from and partnering with the renewable energy industry", Journal of Energy Storage, pp. 311-319, 2018.
[7] M. Hannan, A. Hoque, A. Mohamed, and A. Ayob. "Review of energy storage systems for electric vehicle applications: Issues and challenges", Renewable and Sustainable Energy Reviews, pp.771-789, 2017.
[8] F. Sorgulu, and I. Dincer. "Thermodynamic analyses of a solar-based combined cycle integrated with electrolyzer for hydrogen production", International Journal of Hydrogen Energy, vol. 43, pp. 1047-1059, 2018.
[9] N. Moradi, E. Baniasadi, E. Afshari, and N. Javani. "Performance assessment of a solar hydrogen and electricity production plant using high temperature PEM electrolyzer and energy storage", International Journal of Hydrogen Energy, vol. 43, pp. 5820-5831, 2018.
[10] S. Mena, L. Fernández-Ramírez, C. García-Vázquez, and F. Jurado. "Electrolyzer models for hydrogen production from wind energy systems", International Journal of Hydrogen Energy, vol. 40, pp. 2927-2938, 2015.
[11] V. Papadopoulos, J. Desmet, J. Knockaert, and C. Develder. "Improving the utilization factor of a PEM electrolyzer powered by a 15 MW PV park by combining wind power and battery storage–Feasibility study", International Journal of Hydrogen Energy, vol. 43, pp. 16468-16478, 2018.
[12] K. Bhuyan, K. Hota, and B. Panda. "Modeling and Simulation of Hybrid Energy System Supplying 3empty set Load and its Power Quality Analysis", International Journal of Renewable Energy Research, vol. 8, pp. 592-603, 2018
[13] I. Dincer, and A. Alzahrani, "Electrolyzers", Comprehensive Energy System, pp. 985-1025, 2018.
[14] S. Islam, I. Dincer, and B.S. Yilbas. "System development for solar energy-based hydrogen production and on-site combustion in HCCI engine for power generation", Solar Energy, pp. 65-77, 2016.
[15] A. Ganguly, D. Misra, and S. Ghosh, "Modeling and analysis of solar photovoltaic-electrolyzer-fuel cell hybrid power system integrated with a floriculture greenhouse", Energy and buildings, pp. 2036-2043, 2010.
[16] P.H. Huang, J.K. Kuo, and Z.D. Wu, "Applying small wind turbines and a photovoltaic system to facilitate electrolysis hydrogen production", International Journal of Hydrogen Energy, pp. 8514-8524, 2016.
[17] F. Khalid, M. Aydin, I. Dincer, and M.A. Rosen, "Comparative assessment of two integrated hydrogen energy systems using electrolyzers and fuel cells", International Journal of Hydrogen Energy, pp. 19836-19846, 2016.
[18] A. Buonomano, F. Calise, M. Accadia, and M. Vicidomini, "A hybrid renewable system based on wind and solar energy coupled with an electrical storage: Dynamic simulation and economic assessment", Energy, pp. 174-189, 2018.
[19] O. Izelu, and S. Oghenevwaire, "A review on developments in the design and analysis of wind turbine drive trains", In 2014 International Conference on Renewable Energy Research and Application (ICRERA). IEEE. pp. 589-594, 2014.
[20] M. Tom, and C. Luis, "Principles of Solar Cell Operation", Solar Cells, pp. 1-25, 2013.
[21] H. Abdelkader,and H. Omar, "Application of Solar Energies to Reinforce the Flow Water of Foggara in the

Adrar Region", International Journal of Smart Grid-ijSmartGrid, vol. 2, pp. 203-208, 2018.

[22] M. Bayindir, and S. Parlak, "Application of reaching law approach to design of sliding mode voltage controller for PV system", In 2014 International Conference on Renewable Energy Research and Application (ICRERA). IEEE, pp. 638-642, 2014.

[23] E. Ozgirgin, Y. Devrim, and A. Albostan, "Modeling and simulation of a hybrid photovoltaic (PV) module-electrolyzer-PEM Fuel cell system for micro-cogeneration applications", International journal of hydrogen energy, pp. 1-7, 2015.

[24] A. Ganguly, D. Misra, and S. Ghosh, "Modeling and analysis of solar photovoltaic-electrolyzer-Fuel cell hybrid power system integrated with a floriculture greenhouse", Energy and buildings, vol. 42, pp. 2036-2043, 2010.

[25] R. Ricci, D. Vitali, and S. Montelpare, "An inno vative wind–solar hybrid street light: develop ment and early testing of a prototype", Interna tional Journal of Low-Carbon Technologies, pp. 420-429, 2014.

[26] M. Adaramola, (Ed.), (2014). Wind turbine technology: Principles and design. CRC Press.

[27] A. Manganhar, A. Rajpar, M. Luhur, S. Samo, and M. Manganhar, "Performance Analysis of a Savonius Vertical Axis Wind Turbine Integrated with Wind Accelerating and Guiding Rotor House", Renewable Energy, pp.1-24, 2019.

[28] L. Melcescu, T. Tudorache, O. Craiu, and M. Po pescu, "Finite element analysis of a wind generator with two counter-rotating rotors", IEEE, pp. 408-413, 2017.

[29] M. Casini, "Small vertical axis wind turbines for energy efficiency of buildings", Journal of Clean Energy Technologies, vol. 4, pp. 56-65, 2016.

[30] A. Bagher, M. Vahid, and M. Mohsen, "Types of Solar Cells and Application", American Journal of Optics and Photonics, pp. 94-113, 2015.